Biophysical Chemistry, 37 (1990) 107–119
Elsevier

BIOCHE 01470

The Glu 2^- ··· Arg 10^+ side-chain interaction in the C-peptide helix of ribonuclease A

Robert Fairman [a], Kevin R. Shoemaker [a,*], Eunice J. York [b], John M. Stewart [b] and Robert L. Baldwin [a]

[a] *Department of Biochemistry, Stanford University School of Medicine, Stanford, CA 94305 and* [b] *Department of Biochemistry, University of Colorado School of Medicine, Denver, CO 80262, U.S.A.*

Received 8 January 1990
Accepted 7 February 1990

Helix formation; Salt bridge; Side-chain interaction

Previous studies have identified Lys 1, Glu 2, and His 12 as the charged residues responsible for the pH-dependent stability of the helix formed by the isolated C-peptide (residues 1–13 of ribonuclease A). Here we examine whether the helix-stabilizing behavior of Glu 2^- results from a Glu 2^- ··· Arg 10^+ interaction, which is known to be present in the crystal structure of ribonuclease A. The general approach is to measure the helix content of C-peptide analogs as a function of three variables: pH (titration of ionizing groups), amino acid identity (substitution test), and NaCl concentration (ion screening test). In order to interpret the results of residue replacement, several factors in addition to the putative Glu 2^- ··· Arg 10^+ interaction have been studied: intrinsic helix-forming tendencies of amino acids; interactions of charged residues with the α-helix macrodipole; and helix-lengthening effects. The results provide strong evidence that the Glu 2^- ··· Arg 10^+ interaction is linked to helix formation and contributes to the stability of the isolated C-peptide helix. NMR evidence supports these conclusions and suggests that this interaction also acts as the N-terminal helix stop signal. The implications of this work for protein folding and stability are discussed.

1. Introduction

The C-peptide (residues 1–13) from RNase A provided the first example of a peptide able to form a short monomolecular helix in aqueous solution [1,2]. pH-dependent side-chain interactions were found to be important in stabilizing the helix [2–4]. As regards protein folding, the side-chain interactions in the C-peptide helix are significant in two respects. First, C-peptide presents a simple model system for detecting and quantitating side-chain interactions that contribute to protein stability but are difficult to isolate in studies of an entire protein. Second, the C-peptide helix may function as an autonomous folding unit: the information needed to specify the helical structure of this unit is largely contained in the C-peptide itself [5]. Consequently, the C-peptide helix could play an important role in the folding process. Side-chain interactions that provide helix termination signals [5,6] are important in defining autonomous folding units, and the C-peptide (or S-peptide) system can be used to study these signals as well.

The side-chain interactions found thus far in the C-peptide helix involve charged groups [2,4,7–

Correspondence address: R.L. Baldwin, Department of Biochemistry, Stanford University School of Medicine, Stanford, CA 94305, U.S.A.

* Present address: Department of Biology, Massachusetts Institute of Technology, Cambridge, MA 02139, U.S.A.

Abbreviations: RNase A, bovine pancreatic ribonuclease A; C-peptide, residues 1–13 of RNase A, terminating in homoserine (Hse) lactone at residue 13; S-peptide, residues 1–20 of RNase A; CD, circular dichroism; $[\theta]_{222}$, mean residue ellipticity at 222 nm.

10]. The charge on the N-terminal residue interacts with the α-helix macrodipole to stabilize or destabilize the helix [9,11]. The naturally occurring N-terminal residue (Lys, charge +2) is helix-destabilizing, whereas succinyl-Ala 1 (charge −1) is helix-stabilizing. Two charged residues, Glu 2^- and His 12^+, close to either end of the helix, are responsible for the strong pH dependence of C-peptide helix stability between pH 2 and 8 [4,7,9]. Glu 2^- might be linked to helix stability in either (or both) of two ways. The charge might interact with the α-helix macrodipole [4,9] or the side chain might interact with Arg 10^+, as suggested by the Glu $2^- \cdots$ Arg 10^+ salt bridge in the crystal structure of RNase A [12,13].

Both pH titration of helix content and substitution by Ala have been used in previous work [4,7,9,10] to assign the primary charged-group effects to Glu 2^- and His 12^+, and to show that these two charged groups act independently of each other. Because only Glu 2 can be studied, pH titration studies alone do not show whether Glu 2^- interacts with the macrodipole or with Arg 10^+; the pK_a of Arg 10 is too high for a satisfactory study. Here we use two other methods, an ion screening test and a more extensive substitution test, both in conjunction with pH titration, to characterize the helix-stabilizing interaction involving Glu 2^-. When applied to Arg 10, substitution yields complex results. The reasons for the complexity are analyzed here, and we show what must be done to follow through with a substitution test. We also perform the substitution analysis with Tyr in place of Phe 8 in order to quantitate better the strength of the Glu $2^- \cdots$ Arg 10^+ salt bridge. Tyrosine allows accurate determination of peptide concentration and Tyr 8 can substitute for Phe 8 with only a small effect on the interaction with His 12^+ [10]. By combining an ion screening test with substitution of Arg 10 by Ala, it is possible to determine whether Arg 10^+ interacts with Glu 2^-. In referring to the Glu $2^- \cdots$ Arg 10^+ interaction, the term 'ion pair' is used to denote an electrostatic interaction between oppositely charged ions [14], whereas the term 'salt bridge' refers to a hydrogen-bonded ion pair. Similar studies of the helix-stabilizing interactions involving His 12^+ have been reported elsewhere [10].

2. Materials and methods

Peptide synthesis and purification procedures have been described previously [4,9]. Peptide purity was determined by amino acid analysis and FAB mass spectrometry. The sequences of the peptides studied here are given in table 1. Peptide concentration was measured by either the ninhydrin method [15] or tyrosine absorbance [10]. CD and one-dimensional (1D) ^{1}H-NMR methods have also been described [2,4]. CD measurements

Table 1

Sequences of C-peptide analogs

Peptide	Sequence
C-Peptide	K E T A A A K F E R Q H Hse-lactone
RN16	K E T A A A K F L R A H A – NH_2
RN21	acetyl- A E T A A A K F L R A H A – NH_2
RN23	acetyl- A A T A A A K F L R A H A – NH_2
RN28	acetyl- A E T A A A K F L A A H A – NH_2
RN54	acetyl- A A T A A A K F L A A H A – NH_2
RN25	acetyl- A R T A A A K F L E A H A – NH_2
RN26	acetyl- A D T A A A K F L R A H A – NH_2
RN80	acetyl- A E T A A A K Y L R A H A – NH_2
RN121	acetyl- A A T A A A K Y L R A H A – NH_2
RN119	acetyl- A E T A A A K Y L A A H A – NH_2
RN120	acetyl- A A T A A A K Y L A A H A – NH_2
RN84	acetyl- A E T A E A K Y L R A H A – NH_2

were made on an Aviv 60DS spectropolarimeter in our laboratory, and on a Jasco J-500A spectropolarimeter in the laboratory of J.T. Yang (University of California Medical School, San Francisco). NMR data were acquired on a General Electric GN-500 spectrometer. NOESY experiments were performed by using the time-proportional phase-incrementation method (TPPI) [16, 17]. The water resonance was suppressed by gated irradiation during a 1.5 s delay; 1024 complex points were collected for each of 512 t_1 values, and 64 scans per t_1 value were accumulated. The spectral width was 5600 Hz in both dimensions. The NOESY spectra were acquired with a mixing time of 400 ms. The t_2 dimension was processed with Lorentzian-to-Gaussian weighting using a Gaussian coefficient of 0.2 while the t_1 dimension was processed with a 20^0 phase-shifted sine bell weighting function. A line-broadening parameter of 15 Hz was used. The data were zero filled in t_1 to yield a final matrix of 2048 real points in both dimensions. Data processing was performed on a VAX 8550 computer using Dr. D. Hare's FTNMR program (Infinity Systems, Seattle, WA). Nonlinear least-squares analysis was used to fit the pH titrations of $[\theta]_{222}$ and chemical shift to the Henderson-Hasselbalch equation.

3. Bases of methods

3.1. Ion screening test for an electrostatic interaction

The principle of the ion screening test is straightforward. Mobile counterions arrange themselves so as to oppose an electric field, as in the Debye-Hückel theory of the activity coefficients of ions in simple electrolyte solutions [18]. A high concentration of mobile counterions produces more effective screening of the field than a low concentration. An important point here is that the ion screening test gives a positive result only when an interaction is both electrostatic in origin and sufficiently long-range to be screenable by mobile counterions.

Consider the interaction $A^- \cdots B^+$, which meets these criteria and affects helix stability. One version of the ion screening test involves a comparison of the pH profiles of helix content at moderate (0.1 M) and high (3.0 M) NaCl concentrations. A positive test means here that the changes in helix content accompanying ionization of A and B are diminished in higher salt. Another version of the ion screening test is made by combining ion screening with substitution. For example, replacing either A^- or B^+ with a more neutral (noninteracting) residue would give nonparallel curves of $[\theta]_{222}$ vs NaCl concentration for the two peptides. Replacement of a residue which either is noninteracting or participates in a nonscreenable interaction would give parallel curves. Both versions of the ion screening test have been successfully used to study charge-dipole interactions in the C-peptide helix [9,11] (K.R. Shoemaker et al., unpublished results).

For our studies here, the useful range of NaCl concentration for the ion screening test is from 0 to 3.0 M. Above 3.0 M NaCl, the curves are nearly parallel for all C-peptide analogs that we have studied and presumably reflect salting-out, or Hofmeister series effects, of NaCl (R. Fairman et al., unpublished results). Below 3.0 M NaCl, the ion screening test is strictly a comparison test only; a molecular interpretation of any single salt dependence curve is difficult, since many variables may be involved.

3.2. Measurement of changes in intrinsic helix-forming tendency

In substituting one residue by another, or in titrating an ionizable residue, it is necessary to take account of the changes in intrinsic helix-forming tendency of the residues involved [10]; these changes occur in addition to effects of making or breaking a particular side-chain interaction. The intrinsic helix-forming tendency of an amino acid is reflected in s, the helix growth parameter of the Zimm-Bragg model for α-helix formation [19]. Values of s for nearly all 20 amino acids have been experimentally obtained from host-guest experiments [20,21], and Scheraga [22] has pointed out that they must be combined with position-dependent effects in considering an α-helix with a specific sequence. A change in s alone is likely to cause a measurable change in helix content. This

effect has been studied [23] by making the substitution Ala → Gly at each of five different positions in peptide RN21: the results show that a large drop in helix content results from making this substitution, which is characterized by a particularly large change in s, at any of three interior positions. Marqusee et al. [24] found that short alanine-based peptides form stable helices, a result which cannot be explained by the host-guest parameters for alanine. Therefore, the s values determined by the host-guest method may be context-dependent and may not be applicable to the C-peptide analogues studied here.

4. Results

4.1. Glu 2$^-$ has a charged-group effect on helix stability

Shoemaker et al. [4] identified Glu 2$^-$ as the major residue responsible for the acid limb in a pH titration of helix content for C-peptide. Fig. 1 shows the pH titration of helix content for RN21, the reference peptide (see table 1 for the sequence of this and other peptides). It is clear that Glu 2$^-$ is involved in a helix-stabilizing interaction: no other residue titrates between pH 2 and 5. Moreover, this effect of titrating Glu 2 is dependent on the amount of helix content. There is a decrease in the change in helix content resulting from Glu 2 titration as helix stability decreases, caused either by increasing the temperature or by making a helix-destabilizing replacement (AcAla 1 → Lys 1). The next step is to identify the interaction involving Glu 2$^-$ that gives rise to the charged-group effect.

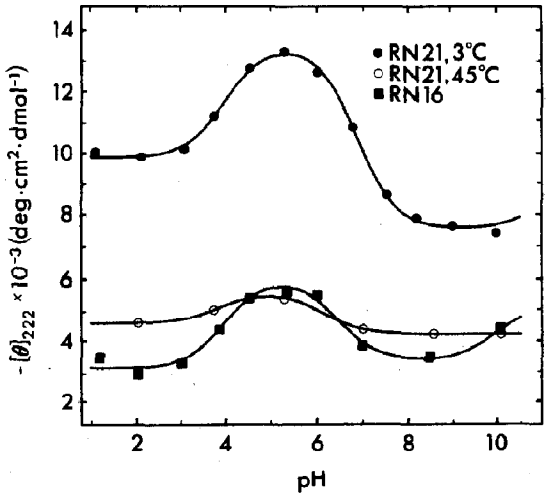

Fig. 1. pH dependence of $[\theta]_{222}$ at 0.1 M NaCl, 3° C, for peptides RN21 and RN16 and at 45° C for peptide RN21. The peptide RN16 contains the substitution AcAla 1 → Lys 1; its pH profile illustrates the effect of a helix-destabilizing substitution on measurement of the Glu 2$^-$ charged-group effect.

4.2. Initial substitution tests for a Glu 2$^-$ ··· Arg 10$^+$ interaction

Substitution analysis has been used to test for the existence of a Glu 2$^-$ ··· Arg 10$^+$ interaction. Fig. 2a shows pH titrations of helix content for RN21, the reference peptide, and for three peptides in which either Glu 2 or Arg 10 or both have been replaced by Ala. We have repeated the substitution analysis with peptides in which Phe 8 has been replaced by Tyr so that we can quantitate these effects better. The results are shown in fig. 2b. Qualitatively, the results are identical. However, RN121 (Y8, R10, A2) and RN120 (Y8, A10, A2) both have higher helix contents than the corresponding peptides that contain F8. This effect may result from the vagaries of the ninhydrin method of concentration determination.

In an Arg 10$^+$ background, the replacement Glu 2 → Ala (RN21 → RN23) leads to a large drop in helix content at pH 5.3 and the acidic limb of the titration curve disappears. Since this result does not distinguish a Glu 2$^-$ ··· dipole interaction from a Glu 2$^-$ ··· Arg 10$^+$ interaction, the key test comes in considering the effects of the replacement Arg 10 → Ala in a Glu 2$^-$ background (RN21 → RN28). For RN28, there is no change in helix content as Glu 2$^-$ is titrated, providing strong evidence that Glu 2$^-$ and Arg 10$^+$ do interact. The change in helix content caused by ionization of His 12 is nearly unaffected by this replacement. Unlike RN21 → RN23, however, there is no significant change in helix content at pH 5.3 for RN21 → RN28. In order to understand this initially puzzling result, several variables in addition to a Glu 2$^-$ ··· Arg 10$^+$ interac-

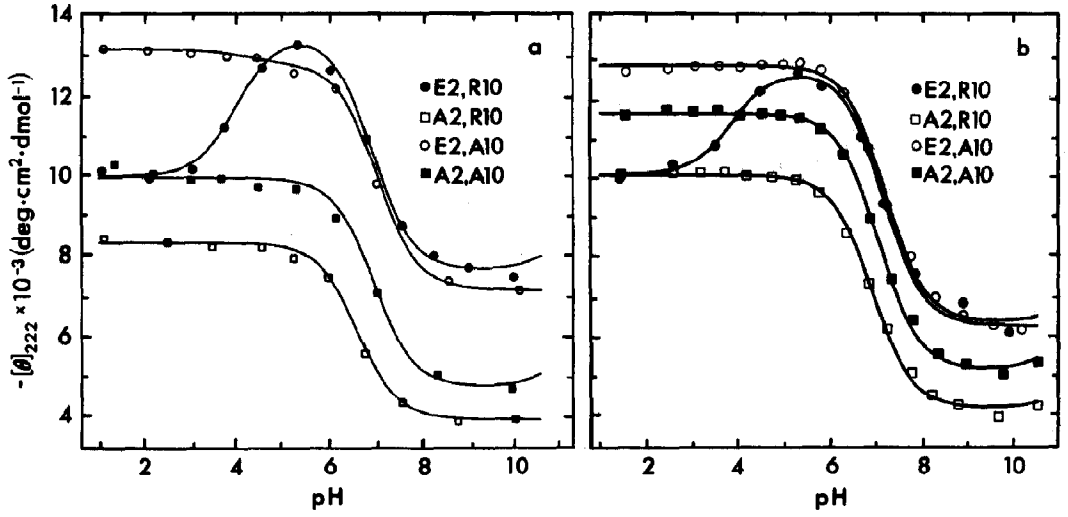

Fig. 2. pH dependence of $[\theta]_{222}$ at 3°C, 0.1 M NaCl, for (a) peptides RN21 (E2, R10), RN23 (A2, R10), RN28 (E2, A10), and RN54 (A2, A10) and (b) peptides RN80 (Y8, E2, R10), RN119 (Y8, E2, A10), RN120 (Y8, A2, A10), and RN121 (Y8, A2, R10).

tion must be considered: (1) differences in intrinsic helix-forming tendency between Arg and Ala, and between Glu and Ala; (2) a Glu 2^- ··· dipole interaction, especially important in an Ala 10 background; and (3) possible helix lengthening when the Glu 2^- ··· Arg 10^+ interaction is broken. Each of these variables will now be considered. Peptide RN54, with both Ala 2 and Ala 10, is the reference for this analysis (fig. 2a).

4.3. *Intrinsic helix-forming tendencies*

As studied in the C-peptide helix, the intrinsic helix-forming tendency of Arg 10^+ is lower than that of Ala 10. This conclusion is reached by noting that the replacement Arg 10 → Ala increases helix content in an Ala 2 background in both the examples shown here (RN23 and RN54 in fig. 2a and RN 120 and RN 121 in fig. 2b) and in pairs of other C-peptide analogs: it does not depend on groups near or at the N-terminus (K.R. Shoemaker et al., unpublished results).

Substitution analysis at several noninteracting positions in the C-peptide helix, combined with pH titration, indicates the following order of intrinsic helix-forming tendencies, which is independent of salt concentration: Glu^0 > Ala > Glu^- (R. Fairman, unpublished results). This rank order agrees well with host-guest s values [25]. These differences are also important in considering the Glu 2^- ··· dipole interaction, as discussed next.

4.4. *Glu 2^- ··· dipole interaction*

The Glu 2^- ··· dipole interaction is most conveniently studied in an Ala 10 background, to eliminate interference from the competing interaction between Glu 2^- and Arg 10^+. Ion screening tests for a Glu 2^- ··· dipole interaction are shown in fig. 3. In these tests, peptide RN28, with Glu 2, is compared to RN54, the control peptide with Ala 2. As seen in fig. 3a, the effect of Glu 2 ionization on helix content varies with salt concentration. The simplest interpretation of these results is that there is a helix-stabilizing Glu 2^- ··· dipole interaction, which must be considered together with the difference in intrinsic helix-forming tendency of Glu^0 and Glu^- discussed above. This difference between Glu 2^- and Glu 2^0 is evident in 3.0 M NaCl, where the Glu 2^- ··· dipole interaction is significantly screened. At lower salt concentrations, the dipole interaction strengthens, becoming larger relative to the effect of intrinsic helical tendency; in 0.01 M NaCl, there is a slight increase in helix content as Glu 2 ionizes. The demonstration of intrinsic helix-

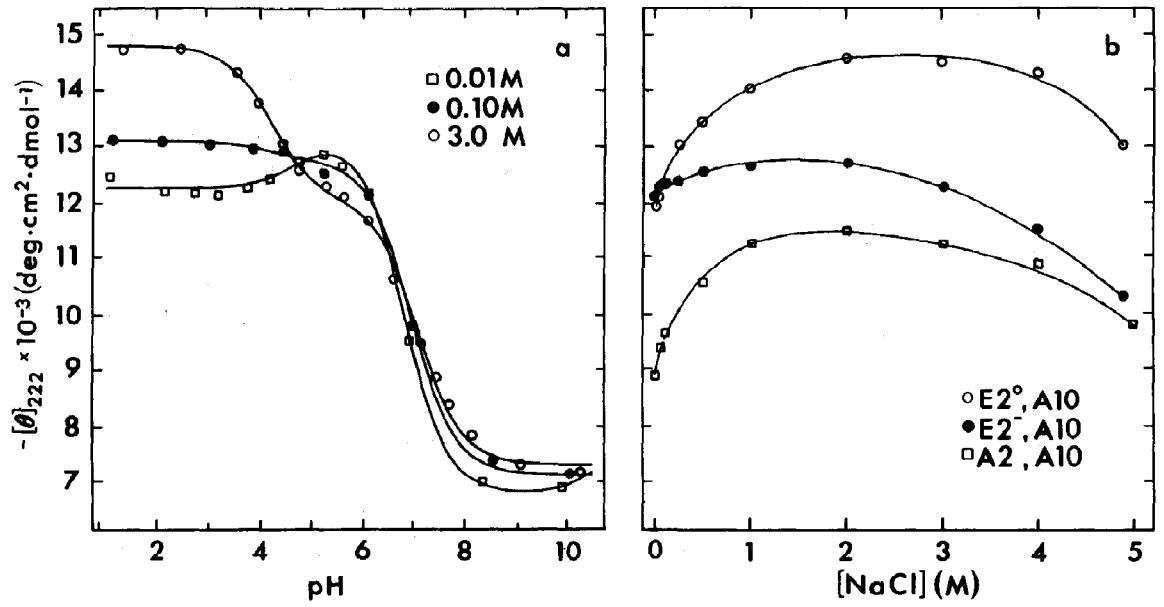

Fig. 3. (a) pH dependence of $[\theta]_{222}$ at 3°C for peptide RN28 (E2, A10) in 0.01, 0.1 and 3.0 M NaCl. (b) NaCl dependence of $[\theta]_{222}$ at 3°C for peptide RN28 (E2, A10), pH 2.0 and 5.3, and peptide RN54 (A2, A10), pH 5.3.

stabilizing effects for Glu 2^0 and Glu 2^- in RN28 strongly suggests that Glu 2 is included in the helix in peptides with Arg 10 → Ala, in agreement with the NMR results on helix lengthening discussed below.

These conclusions are consistent with the ion screening curves for RN28 and RN54 which are shown in fig. 3b. The curves for RN28 at pH 5.3 (Glu 2^-) and pH 2.0 (Glu 2^0), as well as those at pH 5.3 for RN28 (Glu 2^-) and RN54 (Ala 2), are not parallel, indicating that Glu 2^- participates in a screenable electrostatic interaction. The curves for RN28 at pH 2 (Glu 2^0) and RN54 (Ala 2) are nearly parallel, indicating that Glu 2^0 is either noninteracting or not screenable.

4.5. Helix lengthening

In the high-resolution crystal structure of RNase A, the constraint on backbone torsional angles provided by the Glu 2^- ··· Arg 10^+ salt bridge produces an effective N-terminal helix stop at Thr 3. In the C-peptide system, the first indication of a helix-lengthening reaction upon disruption of this interaction came from 1D ^{1}H-NMR studies of RN21 and RN28. Chemical shifts for resonances of several side-chain protons are plotted as a function of pH in fig. 4. Chemical shifts for Thr 3, Phe 8, and Leu 9 in RN21 all parallel CD measurements of helix content (cf. fig. 2a), and are thought to reflect changes in helix stability [2,4,6]. Whereas the chemical shifts for Phe 8 and Leu 9 in RN28 also parallel the CD results, those for Thr 3 and the acetyl blocking group no longer do, as Glu 2 ionizes. Thus, these differences between RN21 and RN28 are localized to side-chain protons near the N-terminus, consistent with helix lengthening when Arg 10 → Ala in a Glu 2 background. For RN28, the changes in chemical shifts of acetyl and Thr 3 side-chain resonances as Glu 2 ionizes may then reflect changes in other interactions (e.g., Glu 2^- ··· dipole or intrinsic effects).

Recently, NOEs and coupling constants have been used to locate helix endpoints in a C-peptide analogue [26]. Some observed NOEs between side-chain and back-bone protons (e.g., Thr 3 NH–Ala 6 βCH3 and Thr 3 βCH–Ala 5 NH) are unusual in α-helices, but are consistent with Glu 2^- ··· Arg 10^+ serving as a helix stop. These

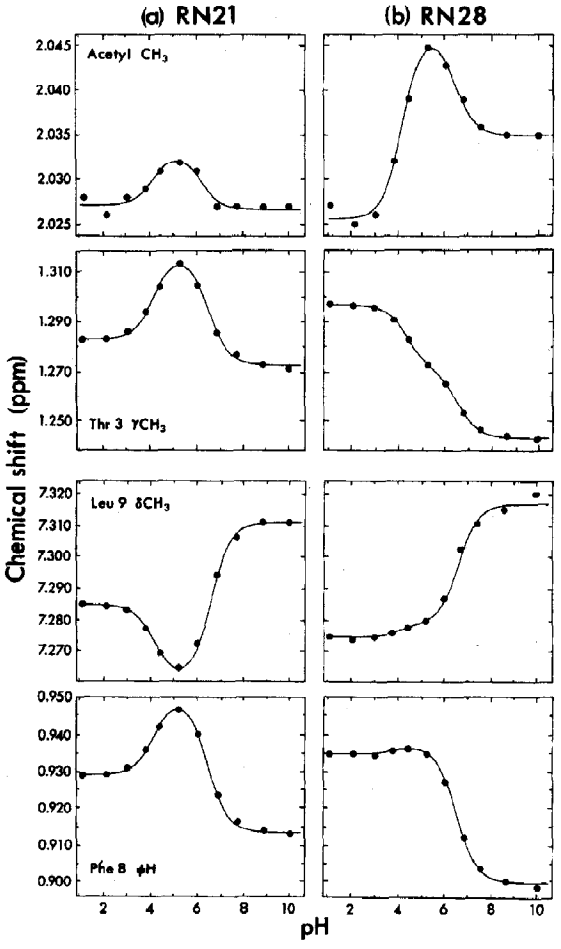

Fig. 4. pH dependence of chemical shift at 3°C, in 0.1 M NaCl, for several side-chain protons in peptides RN21 (a) and RN28 (b). Shown are the CH_3 resonances of the acetyl blocking group, the γCH_3 resonances of Thr 3 (average of two lines), the δCH_3 resonances of Leu 9 (average of four lines), and the ring proton resonances of Phe 8 (average of three lines that shift with helix formation).

NOEs are not observed in peptides with Glu 2 and Ala 10.

4.6. Ion screening of the Glu 2$^-$ ··· Arg 10$^+$ interaction

Next we examine whether the Glu 2$^-$ ··· Arg 10$^+$ ion pair is sensitive to screening by salt. Figs 5 and 6 display the results of ion screening tests. For peptide RN21 in 3.0 M NaCl, there is almost no change in helix content as Glu 2 ionizes, in contrast to the result in 0.1 M NaCl (fig. 5). This result indicates that the Glu 2$^-$ ··· Arg 10$^+$ interaction is effectively screened by mobile counterions. Screening of this interaction is not complete in 3.0 M NaCl, however, as judged by the failure to observe the increase in helicity at pH 2 that is predicted from the intrinsic helix-forming tendencies of Glu 2$^-$ and Glu 2^0 (cf. RN28, with Ala 10, in 3.0 M NaCl: fig. 3a). As Glu 2 ionizes at this higher salt concentration, the increase in helix content accompanying formation of the Glu 2$^-$ ··· Arg 10$^+$ ion pair is approximately cancelled by the decrease in helix content due to the lower intrinsic helix-forming tendency of Glu$^-$.

The salt dependences of helix content for peptides RN21, RN23, and RN28 also suggest the existence of a screenable electrostatic interaction between Glu 2$^-$ and Arg 10$^+$. Fig. 6a gives these results for RN21 and RN23, where the ion screening test is applied to Glu 2 now in the presence of Arg 10$^+$. The curves for RN21 at pH 2 (Glu 2^0) and RN23 (Ala 2) are parallel, indicating that Glu 2^0 is either noninteracting or not screenable (cf. RN28, with Ala 10, at pH 2: fig. 3b). Glu 2$^-$, however, stabilizes the helix via an electrostatic interaction, as shown by the nonparallel curves for RN21 at pH 5.3 (Glu 2$^-$) and pH 2.0 (Glu 2^0), as

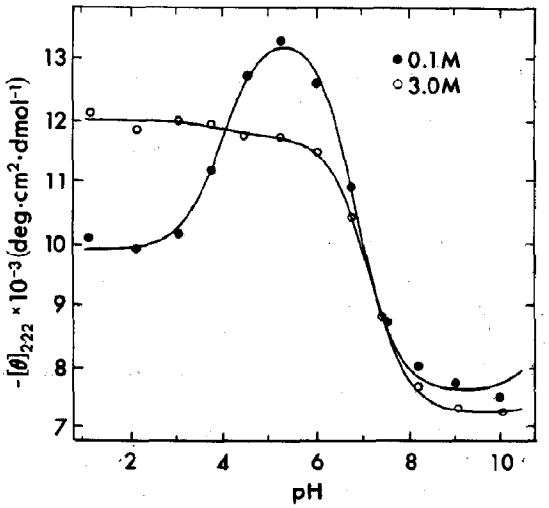

Fig. 5. pH dependence of $[\theta]_{222}$ at 3°C for peptide RN21 in 0.1 and 3.0 M NaCl.

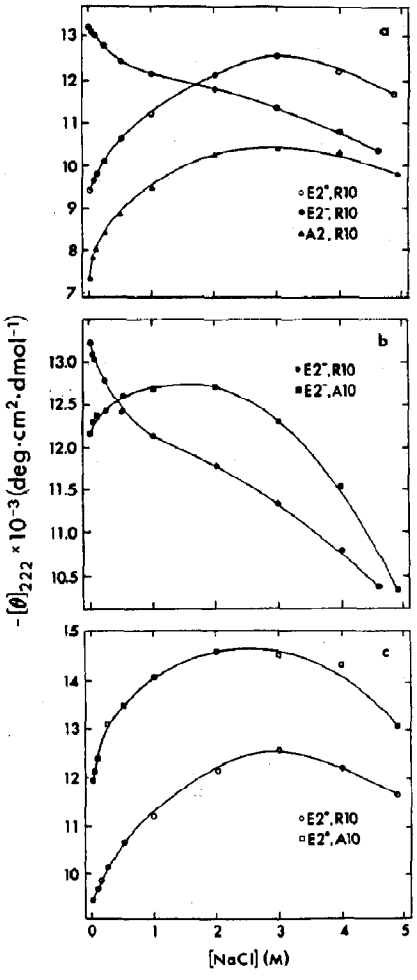

Fig. 6. NaCl dependence of $[\theta]_{222}$ at 3° C. (a) Peptide RN21 (E2, R10) at pH 2.0 and 5.3, and peptide RN23 (A2, R10) at pH 5.3. (b) Peptides RN21 (E2, R10) and RN28 (E2, A10) at pH 5.3. (c) Peptides RN21 and RN28 at pH 2.0.

well as those at pH 5.3 for RN21 (Glu 2^-) and RN23 (Ala 2). The same ion screening test applied to Arg 10^+ in the presence of Glu 2^- is also positive, as shown by the results for RN21 and RN28 given in fig. 6b. The nonparallel salt curves for RN21 (Arg 10^+) and RN28 (Ala 10) at pH 5.3 (Glu 2^-) (fig. 6b), and the parallel curves for these peptides at pH 2.0 (Glu 2^0) (fig. 6c), indicate that Arg 10^+ participates in a screenable electrostatic interaction in the presence of Glu 2^-, but not Glu 2^0. In an Ala 2 background, the ion screening test applied to Arg 10^+ is also negative (R. Fairman et al., unpublished results).

4.7. NMR evidence for the Glu 2^- ··· Arg 10^+ interaction

Fig. 7 shows the pH dependences of chemical shifts for various amide protons and for the Arg 10 Nε proton of peptide RN84. Assignments were made by comparison to the assignments for a related peptide (RN24) made by Osterhout et al. [26], and by use of sequential assignments made from 2D NOESY spectra. The titration shift for the Arg 10 Nε proton has a pK_a of about 4.5, in agreement with the pK_a of Glu 2 determined by CD, and is strongly suggestive of charge-stabilized hydrogen-bonding between Glu 2 and Arg 10. This type of downfield titration shift has been attributed to hydrogen-bonding provided that other possible effects, such as ring-current or through-bond effects [27] or helix formation can be excluded. Peptide RN84 provides a favorable system for this NMR study because the peptide shows only a small change in helix content below pH 7.0, as monitored by CD (unpublished results). The effect of helix formation is evident in the

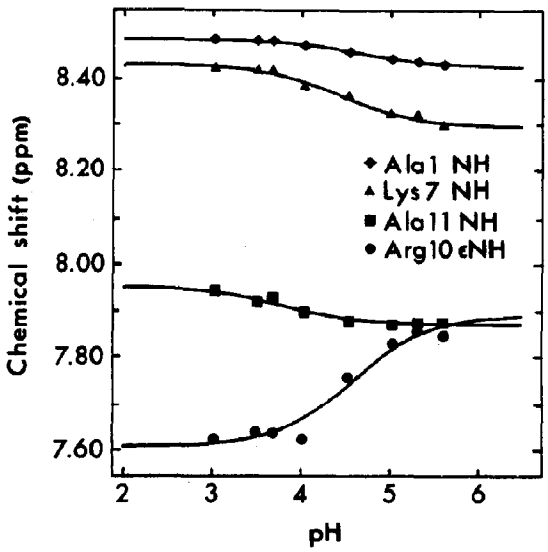

Fig. 7. pH dependence of chemical shift at 3°C, in 0.1 M NaCl, for the amide protons of Ala 1, Lys 7, and Ala 11, and for the Arg 10 Nε proton.

upfield titration shifts of the amide protons shown. These upfield shifts are small, however, compared to the downfield shift of the Arg 10 Nε proton. In a different C-peptide analogue, Dr. A. Bierzynski (personal communication) has also observed a change in the chemical shift of the Arg 10 Nε proton in the pH range where Glu 2 titrates.

4.8. Other peptides

Finally, two other peptides have been studied in connection with the Glu 2^- ··· Arg 10^+ interaction. The effect of shortening the Glu 2 side chain by one methylene group is shown in fig. 8a. The pH profiles of helix content in 0.1 and 3.0 M NaCl for peptide RN26, with Asp 2, are very similar to those for RN21 (cf. fig. 6). Model building indicates that an Asp 2^- ··· Arg 10^+ salt bridge can be made. Inversion of Glu 2 and Arg 10, as in peptide RN25, gives a large drop in helix content (fig. 8b). The reasons for this effect are not clear. The side-chain structure of the helix may interfere with salt-bridge formation after inversion, and inversion probably results in unfavorable interactions of these charged groups with the helix dipole.

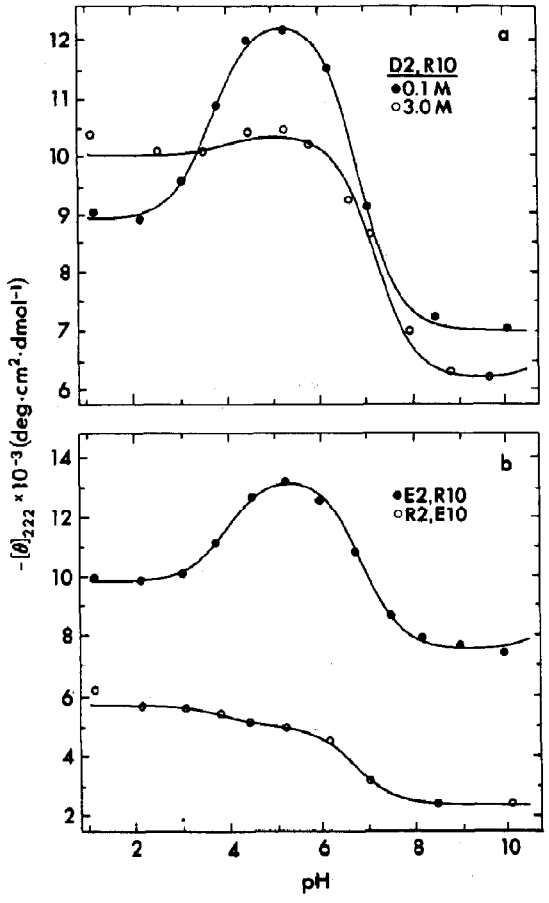

Fig. 8. pH dependence of $[\theta]_{222}$ at 3°C for (a) peptide RN26 in 0.1 and 3.0 M NaCl, and (b) peptides RN21 and RN25 in 0.1 M NaCl.

5. Discussion

5.1. Tests for a Glu 2^- ··· Arg 10^+ interaction

Four pieces of evidence provide the main support for the existence of the Glu 2^- ··· Arg 10^+ salt bridge in the isolated C-peptide helix: (1) the Arg 10 → Ala substitution in a Glu 2 background (fig. 2); (2) the ion screening test applied to Arg 10^+ (fig. 6b and c); (3) NMR studies of peptides with and without Arg 10 in a Glu 2 background (fig. 4 and ref. 26) and (4) the pH dependence of the Arg 10 Nε proton (fig. 7). The NMR result in fig. 7 indicates that Glu 2^- is hydrogen-bonded to Arg 10^+ and therefore that the Glu 2^- ··· Arg 10^+ interaction is a salt bridge. These experiments do not rule out the possibility that some fraction of the RN21 molecules with both Glu 2 and Arg 10 contain a helix-stabilizing Glu 2^- ··· dipole interaction. This fraction, which lacks the Glu 2^- ··· Arg 10^+ salt bridge, might correspond to the 'completely helical conformation' whose presence is deduced from 2D ^{1}H-NMR studies [26].

Substitution analysis of the Glu 2^- ··· Arg 10^+ interaction is not simple, as shown, for example, by the similar helix contents at pH 5.3 for peptides RN21 and RN28 (fig. 2). In order to explain this result, several factors in addition to a Glu 2^- ··· Arg 10^+ interaction have been studied here. The results show that, for the Arg 10 → Ala substitution (RN21 → RN28) in 0.1 M NaCl, the loss in helix content caused by loss of the Glu 2^- ··· Arg 10^+ interaction is compensated by three factors which increase helix content: (1) intrinsic helix-forming tendencies favoring Ala 10

over Arg 10^+; (2) a Glu 2^- ··· dipole interaction, expected to be stronger in an Ala 10 background (fig. 3); and (3) a helix-lengthening reaction to include two more N-terminal residues.

In the studies described here, circular dichroism is used to measure helix content, and does not distinguish between helix stability and helix length. ^{1}H-NMR can, however, be used for this purpose; it has been used previously to localize the helix in S-peptide [3,6]. The NMR results given in fig. 4 indicate that the side-chain conformation at the N-terminus is different after the Glu 2^- ··· Arg 10^+ interaction is broken by the Arg 10 → Ala substitution. These results, taken together with those from recent 2D ^{1}H-NMR experiments [26], provide evidence for a helix-lengthening reaction when this replacement is made. Thus, formation of the Glu 2^- ··· Arg 10^+ salt bridge, unusual in spanning two turns of the helix, requires the peptide backbone to kink at Thr 3 [12] and thereby serves as the N-terminal helix stop signal. The C-terminal helix stop signal [6] has not been identified, although the Phe 8 ··· His 12^+ interaction may be responsible [5,10,26]. A recent example of helix lengthening has been observed in phage T_4 lysozyme: replacement of a proline at the N-terminus of an α-helix resulted in extension of the helix [28].

The high-resolution crystal structure of RNase A clearly indicates that the side chains of Glu 2 and Arg 10 are within hydrogen-bonding distance [12]. Of the experiments shown here, only the pH titration of the chemical shift of the εNH of Arg 10 indicates that the hydrogen-bonded structure is present in the isolated C-peptide. Our experiments do not show whether an interaction between Arg 10^+ and Glu 2^0 persists at low pH, as might be expected for a salt bridge: a singly charge-stabilized hydrogen bond (Glu 2^0 ··· Arg 10^+) could be present at pH 2. The behavior of the side-chain resonance for Thr 3 γCH_3 in RN21 suggests that helix lengthening does not occur with Glu 2^- → Glu 2^0 (cf. RN28, fig. 4), possibly because Glu 2^0 ··· Arg 10^+ does form at low pH (also see ref. 7). If this singly charge-stabilized hydrogen bond is present, it is not detectably screened by mobile counterions, as shown by ion screening tests performed at pH 2 (fig. 6c; cf. ref. 11). More work is needed to resolve these questions. Other studies indicate that singly charge-stabilized hydrogen bonds are stronger than uncharged hydrogen bonds [14,27,29].

5.2. Comparison with other work

Early solution studies supporting the existence of a Glu 2^- ··· Arg 10^+ interaction in ribonuclease S were based on reconstitution of chemically synthesized S-peptide analogues with S-protein to form semisynthetic ribonuclease S [30,31]. 1D ^{1}H-NMR experiments conducted by Rico and co-workers [7,8] are consistent with the conclusion that the Glu 2^- ··· Arg 10^+ interaction plays an important role in the folding of the isolated S-peptide helix.

In RNase A, the Glu 2^- ··· Arg 10^+ salt bridge involves the carboxyl oxygen of Glu 2 and the NH1 and Nε atoms of Arg 10 [12]. This is the most common type of twin nitrogen-twin oxygen interactions, according to a study of the geometries of Glu-Arg pairs in proteins [32]. It is not yet possible to say whether the same geometry is found in the isolated C-peptide helix. ^{1}H-NMR and model-building studies indicate that this type of interaction is also seen in a dipeptide and a tetrapeptide containing an intramolecular Glu^- ··· Arg^+ salt bridge in an organic solvent [33,34].

Statistical analyses of ion pairs in proteins have been made by several workers [35–37]. Although these interactions may be more important in stabilizing tertiary structure than secondary structure [36], their importance in stabilizing α-helices seems clear [14,35,37]. The long central helices seen in the crystal structures of calmodulin [38] and troponin C [39–42] may be stabilized by intrahelical salt bridges. Also, Glu^- ··· Lys^+ salt bridges with an $(i, i+4)$ residue spacing are thought to stabilize helices formed by short, designed peptides [14]. Screening of these interactions with increasing NaCl concentration is observed in the latter study, consistent with the screening of Glu 2^- ··· Arg 10^+ observed here.

Classic studies of several proteins illustrate the importance of ion pairs and salt bridges for protein structure and function: hemoglobin [43], chymotrypsin [44], thermolysin [45], pancreatic

trypsin inhibitor [46], δ-crystallin II [47], ferredoxin [48], neurophysin-hormone interactions [49] and T_4 lysozyme [50]. In several of these cases, the free energy of formation of specific salt bridges has been measured; these energies are larger for a buried salt bridge than for a water-accessible salt bridge, in accord with the lower dielectric constant of the protein interior [51].

5.3. Implications for protein folding

Until recently, it was thought that fragments of single-domain proteins could not fold in aqueous solution. In the few cases where they did, the low amount of structure was considered to be insignificant for directing the folding process (for reviews, see refs 52 and 53). Two conclusions from work on C-peptide and S-peptide are clear: first, isolated peptide helices can form in aqueous solution and second, several features of the protein helix are duplicated in the isolated peptide helix. Does the C-peptide helix represent a fortuitous, isolated exception to the general rule? Although the current data base is still too small to answer this question, there is a growing list of documented cases of secondary structure formation (especially helix and turn) by short peptides in aqueous solution [54–59]; and by a larger peptide model of a BPTI folding intermediate [60].

In the framework model for protein folding [61], the first step in folding is the formation of local secondary structures in the otherwise unfolded polypeptide chain. Next, these elements associate to form a framework, as modelled by the ridge-into-groove helix pairing in myoglobin [62]. In the final stages of folding, side chains are buried as water is excluded from the protein interior. Experiments of the kind discussed here, which clearly establish that short protein fragments can fold in aqueous solution and that their structures are stabilized by local interactions, indicate that the framework model is feasible on energetic grounds. Since interactions involving distant residues may be absent in these early folding intermediates, the relatively low levels of structure shown by these fragments in aqueous solution are not surprising. In fact, the Glu 2^- ··· Arg 10^+ interaction, although energetically small, nevertheless helps to stabilize the helix to a level where it is detectable. We have recently shown that a Phe $8 \cdots$ His 12^+ ring interaction also contributes to the stability of the C-peptide helix [10]. Additional helix-stabilizing side-chain interactions (e.g., hydrophobic interactions) remain to be identified.

Studies of peptide folding and stability provide a novel approach for studying factors involved in protein folding and stability (cf. refs 60 and 63). Our work has pointed out several caveats for these studies. First, characterizing the structures of short peptides will be easier if there is a single dominant folded conformation. Both high-resolution NMR and X-ray crystallography offer the promise of detailed structural analyses in favorable circumstances. Second, amino acid substitution experiments to study one interaction may allow an interacting residue to turn to an alternative interaction when its original partner has been replaced. For example, as studied here, the Arg 10 → Ala substitution strengthens the Glu $2^- \cdots$ dipole interaction. Changes in intrinsic helix-forming tendency which accompany substitution must also be considered. Peptide structures are relatively unstable compared to the folded conformations of proteins, and therefore should be more susceptible to perturbing mutations. Likewise, local interactions which affect the stability of the 'unfolded' (e.g., nonhelical) state [64] may affect the structures formed by peptides more than those of proteins.

5.4. Concluding remarks

The experiments described here show how substitution analysis can be used to determine whether a charged residue (Glu 2^-) increases helix stability primarily by interacting with a second residue (Arg 10^+) or with the α-helix macrodipole. They also illustrate certain pitfalls of substitution analysis and indicate the type of controls needed to evaluate the various effects of residue substitution.

Acknowledgments

We thank Drs Andrew Robertson, Jannette Carey, Peter Kim and Michael Levitt for helpful discussions, Virginia Robbins for technical assis-

tance, and Dr. J.T. Yang for the use of his spectropolarimeter. We thank Leland V. Miller of the NIH Clinical Mass Spectrometry Resource, University of Colorado, for the FAB mass spectra, supported by grant RR01152. This research was supported by grant GM 31475 from the National Institutes of Health.

References

1 J.E. Brown and W.A. Klee, Biochemistry 10 (1971) 470.
2 A. Bierzynski, P.S. Kim and R.L. Baldwin, Proc. Natl. Acad. Sci. U.S.A. 79 (1982) 2470.
3 M. Rico, J.L. Nieto, J. Santoro, F.J. Bermejo, J. Herranz and E. Gallego, FEBS Lett. 162 (1983) 314.
4 K.R. Shoemaker, P.S. Kim, D.N. Brems, S. Marqusee, E.J. York, I.M. Chaiken, J.M. Stewart and R.L. Baldwin, Proc. Natl. Acad. Sci. U.S.A. 82 (1985) 2349.
5 K.R. Shoemaker, R. Fairman, P.S. Kim, E.J. York, J.M. Stewart and R.L. Baldwin, Cold Spring Harbor Symp. Quant. Biol. 52 (1987) 391.
6 P.S. Kim and R.L. Baldwin, Nature 307 (1984) 329.
7 M. Rico, E. Gallego, J. Santoro, F.J. Bermejo, J.L. Nieto and J. Herranz, Biochem. Biophys. Res. Commun. 123 (1984) 757.
8 M. Rico, J. Santoro, F.J. Bermejo, J. Herranz, J.L. Nieto, E. Gallego and M.A. Jiménez, Biopolymers 25 (1986) 1031.
9 K.R. Shoemaker, P.S. Kim, E.J. York, J.M. Stewart and R.L. Baldwin, Nature 326 (1987) 563.
10 K.R. Shoemaker, R. Fairman, D.A. Schultz, A.D. Robertson, E.J. York, J.M. Stewart and R.L. Baldwin, Biopolymers 29 (1990) 1.
11 R. Fairman, K.R. Shoemaker, E.J. York, J.M. Stewart and R.L. Baldwin, Proteins 5 (1988) 1.
12 A. Wlodawer and L. Sjölin, Biochemistry 22 (1983) 2720.
13 A. Wlodawer, L.A. Svensson, L. Sjölin and G.L. Gilliland, Biochemistry 27 (1988) 2705.
14 S. Marqusee and R.L. Baldwin, Proc. Natl. Acad. Sci. U.S.A. 84 (1987) 8898.
15 H. Rosen, Arch. Biochem. Biophys. 67 (1957) 10.
16 G. Drobny, A. Pines, S. Sinton, D. Weitekamp and D. Wemmer, Symp. Faraday Soc. 186 (1979) 435.
17 D. Marion and K. Wuthrich, Biochem. Biophys. Res. Commun. 113 (1983) 967.
18 P. Debye and E. Hückel, Phys. Z. 24 (1923) 185.
19 B.H. Zimm and J.K. Bragg, J. Chem. Phys. 31 (1959) 526.
20 M. Sueki, S. Lee, S.P. Powers, J.B. Denton, Y. Konishi and H.A. Scheraga, Macromolecules 17 (1984) 148.
21 H.A. Scheraga, Pure Appl. Chem. 50 (1978) 315.
22 H.A. Scheraga, Proc. Natl. Acad. Sci. U.S.A. 82 (1985) 5585.
23 K.G. Strehlow and R.L. Baldwin, Biochemistry 28 (1989) 2130.
24 S. Marqusee, V.H. Robbins and R.L. Baldwin, Proc. Natl. Acad. Sci. U.S.A. 86 (1989) 5286.
25 F.R. Maxfield, J.E. Alter, G.T. Taylor and H.A. Scheraga, Macromolecules 8 (1975) 479.
26 J.J. Osterhout, R.L. Baldwin, E.J. York, J.M. Stewart, H.J. Dyson and P.E. Wright, Biochemistry 28 (1989) 7059.
27 A. Bundi and K. Wüthrich, Biopolymers 18 (1979) 299.
28 T. Alber, J.A. Bell, S. Dao-Pin, H. Nicholson, J.A. Wozniak, S. Cook and B.W. Matthews, Science 239 (1988) 631.
29 A.R. Fersht, J.-P. Shi, J. Knill-Jones, D.M. Lowe, A.J. Wilkinson, D.M. Blow, P. Brick, P. Carter, M.M.Y. Waye and G. Winter, Nature 314 (1985) 235.
30 K. Hofmann, J.P. Visser and F.M. Finn, J. Am. Chem. Soc. 92 (1970) 2900.
31 F. Marchiori, G. Borin, L. Moroder, R. Rocchi and E. Scoffone, Biochim. Biophys. Acta 257 (1972) 210.
32 J. Singh and J.M. Thornton, FEBS Lett. 228 (1988) 357.
33 G. Lancelot, R. Mayer and C. Helene, J. Am. Chem. Soc. 101 (1979) 1569.
34 R. Mayer and G. Lancelot, J. Am. Chem. Soc. 103 (1981) 4738.
35 F.R. Maxfield and H.A. Scheraga, Macromolecules 8 (1975) 491.
36 D.J. Barlow and J.M. Thornton, J. Mol. Biol. 168 (1983) 867.
37 M. Sundaralingam, Y.C. Sekharudu, N. Yathindra and V. Ravichandran, Proteins 2 (1987) 64.
38 Y.S. Babu, J.S. Sack, T.J. Greenhough, C.E. Bugg, A.R. Means and W.J. Cook, Nature 315 (1985) 37.
39 M. Sundaralingam, W. Drendel and M. Greaser, Proc. Natl. Acad. Sci. U.S.A. 82 (1985) 7944.
40 K.A. Satyshur, S.T. Rao, D. Pyzalska, W. Drendel, M. Greaser and M. Sundaralingam, J. Biol. Chem. 263 (1988) 1628.
41 O. Herzberg and M.N.G. James, Nature 313 (1985) 653.
42 O. Herzberg, J. Moult and M.N.G. James, in: Calcium and the cell: Ciba Foundation Symposium 122, eds. D. Evered, and J. Whelan (Wiley, Chichester, 1986) p. 120.
43 M.F. Perutz, G. Fermi, B. Luisi, B. Shaanan and R.C. Liddington, Acc. Chem. Res. 20 (1987) 309.
44 A.R. Fersht, J. Mol. Biol. 64 (1972) 497.
45 P.M. Colman, J.N. Jansonius and B.W. Matthews, J. Mol. Biol. 70 (1972) 701.
46 L.R. Brown, A. DeMarco, R. Richarz, G. Wagner and K. Wüthrich, Eur. J. Biochem. 88 (1978) 87.
47 T.L. Blundell, P. Lindley, L. Miller, D. Moss, C. Slingsby, I. Tickle, W. Turnell and G. Wistow, Nature 289 (1981) 771.
48 M.F. Perutz and H. Raidt, Nature 255 (1975) 256.
49 E. Breslow and P. Gargiulo, Biochemistry 16 (1977) 3397.
50 D.E. Anderson, W.J. Becktel and F.W. Dahlquist, Biochemistry 29 (1990) 2403.
51 J.B. Matthew, Annu. Rev. Biophys. Biophys. Chem. 14 (1985) 387.
52 D.B. Wetlaufer and S. Ristow, Annu. Rev. Biochem. 42 (1973) 135.

53 D.B. Wetlaufer, Adv. Protein Chem. 34 (1981) 61.
54 H.J. Dyson, K.J. Cross, R.A. Houghten, I.A. Wilson, P.E. Wright and R.A. Lerner, Nature 318 (1985) 480.
55 H.J. Dyson, M. Rance, R.A. Houghten, R.A. Lerner and P.E. Wright, J. Mol. Biol. 201 (1988) 161.
56 H.J. Dyson, M. Rance, R.A. Houghten, P.E. Wright and R.A. Lerner, J. Mol. Biol. 201 (1988) 201.
57 C. Boesch, A. Bundi, M. Oppliger and K. Wüthrich, Eur. J. Biochem. 91 (1978) 209.
58 A. Bundi, R.H. Andreatta and K. Wüthrich, Eur. J. Biochem. 91 (1978) 201.
59 E.M. Goodman and P.S. Kim, Biochemistry 28 (1989) 4343.
60 T.G. Oas and P.S. Kim, Nature 336 (1988) 42.
61 P.S. Kim and R.L. Baldwin, Annu. Rev. Biochem. 51 (1982) 459.
62 C. Chothia, M. Levitt and D. Richardson, J. Mol. Biol. 145 (1981) 215.
63 C. Mitchinson and R.L. Baldwin, Proteins 1 (1986) 23.
64 D.P. Goldenberg, J. Cell. Biochem. 29 (1985) 321.